Lifetime measurements in the transitional nucleus ^{138}Gd

M. G. Procter,[1] D. M. Cullen,[1] P. Ruotsalainen,[2] T. Braunroth,[3] A. Dewald,[3] C. Fransen,[3] T. Grahn,[2] P. T. Greenlees,[2] M. Hackstein,[3] K. Hauschild,[2] U. Jakobsson,[2] P. M. Jones,[2] R. Julin,[2] S. Juutinen,[2] S. Ketelhut,[2] A. Lopez-Martens,[2] M. Leino,[2] J. Litzinger,[3] P. J. R. Mason,[4] P. Nieminen,[2] P. Peura,[2] P. Rahkila,[2] M. W. Reed,[4] S. Rice,[4] S. Rinta-Antilla,[2] W. Rother,[3] M. Sandzelius,[2] J. Sarén,[2] C. Scholey,[2] J. Sorri,[2] M. J. Taylor,[1] J. Uusitalo,[2] A. Vitturi,[5] Y. Shi,[6] and F. R. Xu[6]

[1]*Schuster Laboratory, University of Manchester, Manchester, M13 9PL, United Kingdom*
[2]*Department of Physics, University of Jyväskylä, FIN-40014 Jyväskylä, Finland*
[3]*Institut für Kernphysik, Universität zu Köln, D-50937, Köln, Germany*
[4]*Department of Physics, University of Surrey, Guildford, GU2 5XH, United Kingdom*
[5]*Physics Department and INFN, via Marzolo 8, I-35131 Padova, Italy*
[6]*Department of Technical Physics, Peking University, Beijing 100871, China*

(Received 4 July 2011; published 17 August 2011)

Lifetime measurements have been made in the ground-state band of the transitional nucleus ^{138}Gd from coincidence recoil-distance Doppler-shift data. ^{138}Gd nuclei were produced using the ^{106}Cd (^{36}Ar, $2p2n$) reaction with a beam energy of 190 MeV. Reduced transition probabilities have been extracted from the lifetime data collected with the Köln plunger placed at the target position of the JUROGAM-II array. The $B(E2)$ values have been compared with predictions from X(5) critical-point calculations, which describe the phase transition between vibrational and axially symmetric nuclear shapes, as well as with IBM-1 calculations at the critical point. While the excitation energies in ^{138}Gd are consistent with X(5) predictions, the large uncertainties associated with the measured $B(E2)$ values cannot preclude vibrational and rotational contributions to the low-lying structure of ^{138}Gd. Although experimental knowledge for the low-lying γ and β-vibrational bands in ^{138}Gd is limited, potential-energy surface calculations suggest an increase in γ softness in the ground-state band. In order to more fully account for the effects of γ softness, the X(5) and IBM-1 calculations need to be extended to include the γ degree of freedom for ^{138}Gd.

DOI: 10.1103/PhysRevC.84.024314 PACS number(s): 21.10.Tg, 21.60.−n, 23.20.−g, 27.60.+j

I. INTRODUCTION

Critical-point symmetries provide an elegant way of describing transitional nuclei which reside at the intermediate points between extremes of nuclear structure [1–3]. Iachello has analytically derived two critical-point symmetries using a parameter-free (except for scale) prescription with the five-dimensional Bohr Hamiltonian [4,5]. In this model, the critical-point symmetries describe the second-order phase transition between sphericity and a γ-unstable rotor, E(5) [4], and the first-order phase transition from sphericity to an axially deformed nuclear shape, X(5) [5]. For X(5) symmetry, the potential is modeled as a square well in the β degree of freedom and an axially symmetric potential in the γ degree of freedom (a harmonic oscillator with a minimum at $\gamma^\circ = 0$). The ability to decouple the β and γ degrees of freedom in this model initially allowed the equations governing the excited states at the critical point to be solved [5].

To date, experimental evidence to support an X(5) description of transitional nuclei has been mainly limited to the $N = 90$ isotones. Several characteristic examples of X(5) behavior have been found in these nuclei, for example, ^{152}Sm [6] and ^{150}Nd [7]. The possible existence of critical-point behavior in nuclei can be inferred from the so-called P factor [8]. This P factor aims to describe the competing effects between the deformation-driving proton-neutron (p-n) interaction and the $L = 0$ coupled, sphericity-driving pairing interaction as a function of the number of valence nucleons [9]. A value of $P \sim 5$, which many of the $N = 90$ isotones show, describes the point at which the p-n interaction just begins to dominate. Values of $P \sim 5$ are also observed for a variety of rare-earth nuclei. For example, recent measurements have been performed to assess the possible X(5) behavior in ^{130}Ce [10]. In that work, however, discrepancies between the experimentally measured reduced transition probabilities and those expected based upon the X(5) model were found. These differences were attributed to the effects of the γ degree of freedom; ^{130}Ce was deduced to be softer, with respect to γ distortions, than the axially symmetric potential used in the X(5) calculations [10].

In order to expand the knowledge of the X(5) critical-point behavior in the $A \sim 130$ region of the nuclear chart, ^{138}Gd has been studied. ^{138}Gd, with 14 valence protons and 8 valence neutron holes, has a value of $P \sim 5.1$. Additionally, the experimentally measured energy ratio of the first excited 2^+ and 4^+ states, $R_{4/2} = 2.74$ [11], is reasonably close to the value of 2.91 predicted for X(5) [5]. In order to determine whether ^{138}Gd lies at the X(5) critical point, experimentally measured electromagnetic transition strengths should be compared with theoretically predicted values based upon different macroscopic models of the nuclear shape. To examine the proposed X(5) behavior of the nucleus ^{138}Gd in this work, reduced transition probabilities have been determined from lifetime measurements made with the recoil-distance Doppler-shift (RDDS) technique. Previously, using the recoil distance method with a thick gold stopper foil, Bishop *et al.* [12] extracted lifetimes for the first three excited levels in the yrast sequence in ^{138}Gd. However, those measurements were not sensitive to the absolute feeding properties of higher lying states, or indeed to any contributions from unobserved

side feeding. This was a consequence of the small number of germanium detectors used in the experiment; in order to account for the contributions of higher lying states toward the lifetimes of those being measured, assumptions had to be placed on the lifetimes of the feeding states [12]. These assumptions were noted to have a significant effect on the final lifetime values. The present work has aimed to improve upon previous results by remeasuring these lifetimes, and those of the higher-spin states in the ground-state band, using γ-ray coincidences. With γ-ray coincidences, the complications from unobserved feeding are removed, and the lifetime of the excited state can be determined without systematic errors arising from feeding assumptions. In this work, the $B(E2)$ values have been extracted from the lifetime measurements of the four lowest members of the ground-state band in ^{138}Gd. The $B(E2)$ values have been compared with theoretical calculations based upon the X(5) model as well as to an interacting boson approximation (IBA) fit and those predicted by potential-energy surface (PES) calculations.

II. EXPERIMENTAL METHODS AND DATA ANALYSIS

Excited states in ^{138}Gd were populated using the ^{106}Cd (^{36}Ar, $2p2n$) reaction at a beam energy of 190 MeV at the accelerator laboratory of the University of Jyväskylä, Finland. Prompt γ-ray decays were observed in the JUROGAM II spectrometer [13] located around the target chamber. The recoil-ion transport unit (RITU) [14,15] transported the recoiling nuclei to the gamma recoil electron alpha tagging (GREAT) focal plane spectrometer [16], where they were implanted into a pair of double-sided silicon strip detectors (DSSDs) [17].

In order to allow the collection of RDDS data, the Köln plunger [18] was placed at the center of the JUROGAM II spectrometer. This housed both a 0.6-mg/cm^2 ^{106}Cd target and a downstream 1.06-mg/cm^2 Mg degrader foil to reduce the recoiling velocity of the ^{138}Gd nuclei from $v/c = 0.029(2)$ to 0.016(2). Data were collected at nine target-to-degrader distances of 15.77(3), 21.68(4), 29.7(3), 54.2(2), 98.54(2), 197.1(2), 1000(3), 1500(5), and 2000(6) μm. To facilitate the collection of data at very small target-to-degrader separations, both the target and degrader foils were stretched. The known difficulties associated with stretching a cadmium target required it to be mounted onto a forward-facing 1.7-mg/cm^2 Ta foil. Consequently, excited nuclear states were produced from the Coulomb excitation of tantalum nuclei with a large cross section. In order to remove the Coulomb excitation events from the data, it was necessary to employ the method of recoilgating. Typically, the GREAT DSSD is used to tag on implanted recoiling nuclei; however, due to the low Q value associated with the heavy-ion fusion-evaporation reaction, recoiling compound nuclei were produced with insufficient energy to traverse the full length of RITU; The majority deposited the full amount of their remaining kinetic energy in the Multiwire Proportional Counter (MWPC) at the entrance to GREAT. In order to maintain the typical recoil-tagging conditions provided by this setup, the MWPC was used to identify recoiling nuclei by increasing the gas pressure and amplifier gains.

Data were time stamped by a 100-MHz clock from the Total Data Readout (TDR) acquisition system [19] and collected online using the GRAIN software package [20]. The data were sorted into two-dimensional asymmetric matrices to be analyzed with the UPAK software suite [21]. Matrices were constructed for each target-to-degrader distance from data collected in the combined JUROGAM II rings 3 and 4 (24 clover detectors), located around 90° to the beam axis versus ring 2 (10 single-crystal Ge detectors), at a backward angle of 134°. A Doppler-shift correction was applied to the data.

Lifetime data were analyzed using the differential decay curve method (DDCM) in the γ-ray coincidence mode [22,23]. The final lifetimes were extracted from a weighted average of values determined at specific target-to-degrader distances using

$$\tau(x) = \frac{\{C, A_d\} - \alpha\{C, B_d\}}{\frac{d}{dx}\{C, A_s\}} \frac{1}{\langle v \rangle}. \quad (1)$$

The terms A and B correspond to the Doppler shifted (s) and degraded (d) peaks of the transitions depopulating and feeding the state of interest, respectively. The intensities were determined from coincidence gates placed upon the higher lying transition(s), C. The α term takes into consideration the difference in intensities of the transitions feeding and depopulating the state being measured. The final measurements were determined from individual lifetime values that lie within the so-called region of sensitivity. These values are the most sensitive to the lifetime of the nuclear state and can be found with the smallest error when both the numerator and denominator in Eq. (1) are maximized. It is expected that within this region the individual lifetimes at each target-to-degrader distance should remain constant, and any deviation from this trend is indicative of systematic errors in the setup. Typically, coincident gates are placed solely upon the Doppler-shifted component of the photo peak, which has the effect of removing any contributions from nuclear deorientation in the final lifetime value. As a consequence of the limited number of JUROGAM II rings available in the experiment, gates were placed on transitions observed in detector rings 3 and 4 around 90° to the beam axis. The poor separation of the two components of each transition at such angles necessitated gating across the full width of the photo peaks. The presence of nuclear deorientation effects in this approach is common to both the feeding and depopulating γ-ray transitions. These effects can be removed by the inclusion of the decay properties of the feeding transition in the calculation of the lifetime [24], as expressed in Eq. (1); that is, gates were not placed directly on the feeding transition. It should also be noted that within the DDCM, it is only the relative target-to-degrader distances that are of importance, not the absolute values.

III. RESULTS

In this work, lifetime measurements have been made for the four lowest-spin states in the yrast band of ^{138}Gd; see Fig. 1. Lifetimes were determined from observing the ratio of the fully Doppler-shifted and degraded peaks from data collected

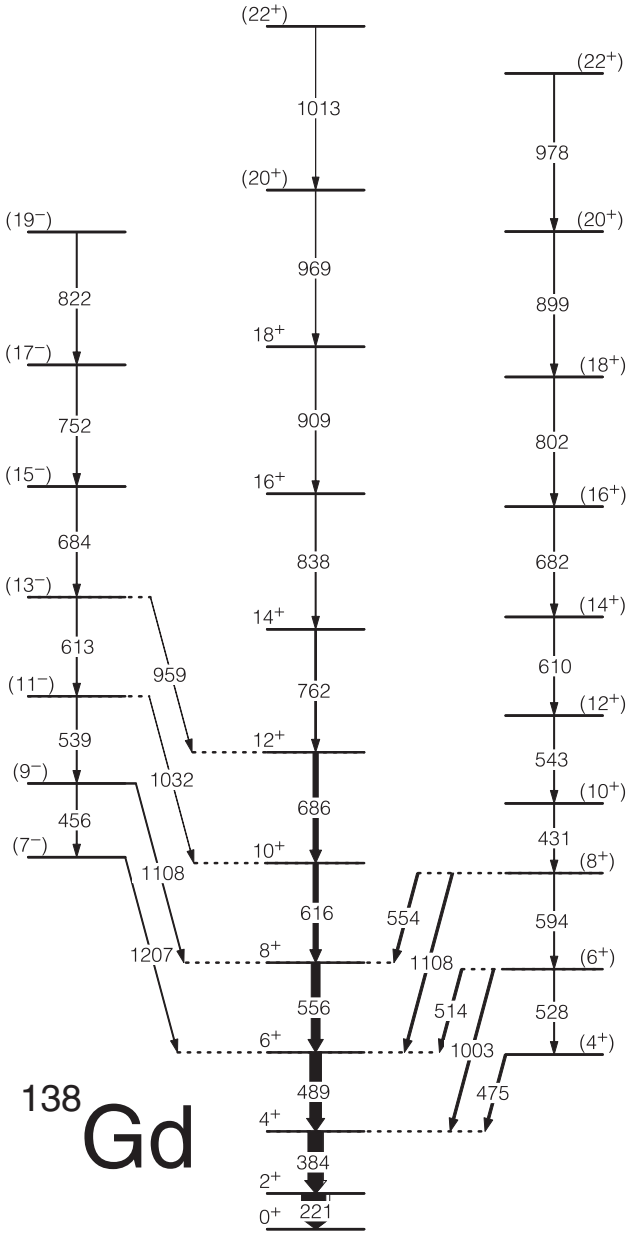

FIG. 1. Partial level scheme of ^{138}Gd taken from Ref. [25]. The widths of the arrows correspond to the intensities of each transition.

in ring 2 of the JUROGAM II array at a backward angle of 134° to the beam line, after setting gates on higher lying transitions in the combined rings 3 and 4 around 90° to the beam axis. Figure 2 shows an example of the data collected at four target-to-degrader distances for the $2^+ \rightarrow 0^+$ transition in ^{138}Gd. The spectra were obtained from a summation of gates on the higher lying 489-, 556-, and 616-keV transitions. The positions of the fully Doppler-shifted and degraded peaks have been highlighted. The data collected from this summation of gates allowed the calculation of the lifetime for the first excited 2^+ state in ^{138}Gd, shown in Table I. It was not possible to include higher lying gates due to overlapping coincident γ-ray energies in the nuclei ^{137}Sm [26] and ^{139}Gd [27] with ^{138}Gd, which were produced with relative cross sections of 18% and 5%, respectively.

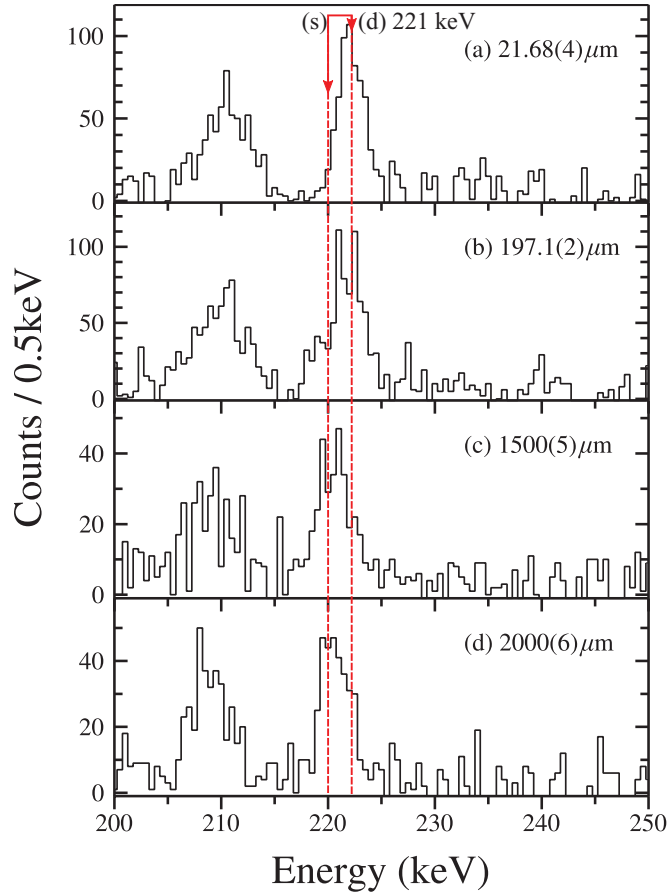

FIG. 2. (Color online) Example of recoil-gated γ-γ coincidence spectra for four target-to-degrader distances for the 221-keV transition in the ground-state band of ^{138}Gd. The spectra were obtained from a summation of gates across the full photo-peak widths of the 489-, 556-, and 616-keV γ rays. The splitting of the fully Doppler-shifted (s) and degraded (d) components is highlighted. The peak to the left of the 221-keV transition in ^{138}Gd is the 209-keV ground-state transition in ^{137}Sm [26].

The lifetime for the first excited 2^+ state has been measured with an improved uncertainty compared with previous measurements and is in good agreement with that measured by Bishop *et al*. [12]. In that work it was assumed that feeding corrections were not required as the 2^+ state was seen to be

TABLE I. Experimentally measured lifetime values τ and branching ratios α for excited yrast states in ^{138}Gd measured in this work and those measured by Bishop *et al*. [12].

$J_i^\pi \rightarrow J_f^\pi$	α	τ (ps), this work	τ (ps), Ref. [12]
$2^+ \rightarrow 0^+$	1.03(2)	308(17)	305(30)
$4^+ \rightarrow 2^+$	0.94(3)	13.3(18)	2.6(20)
$6^+ \rightarrow 4^+$	1.10(10)	3.8(15)	13.7(16)[a]
			7(2)[b]
$8^+ \rightarrow 6^+$	1.08(10)	1.8(4)	—

[a]Fitted with no feeding assumptions.
[b]Fitted with assumption that the preceding state has the same deformation.

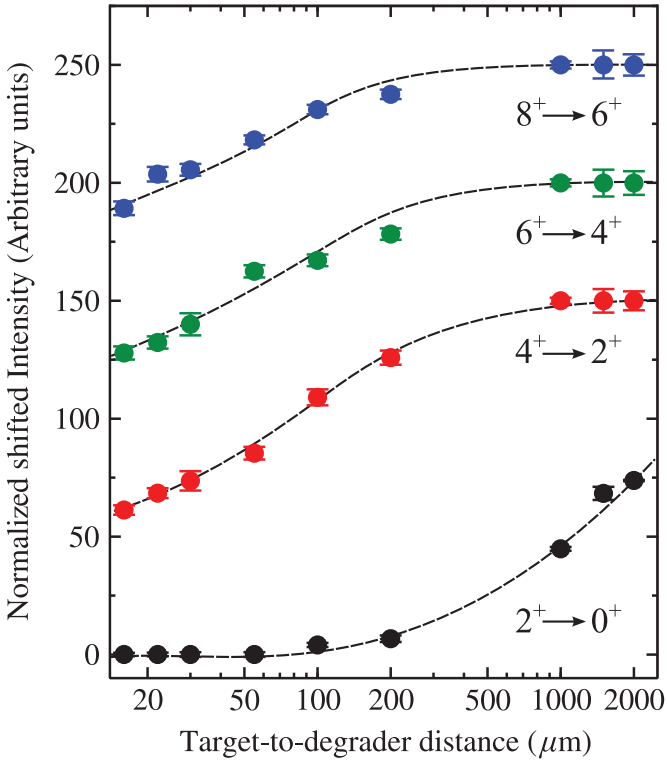

FIG. 3. (Color online) Normalized shifted intensities for the four ground-state transitions in ^{138}Gd measured in this work. The dashed curves are drawn to guide the eye.

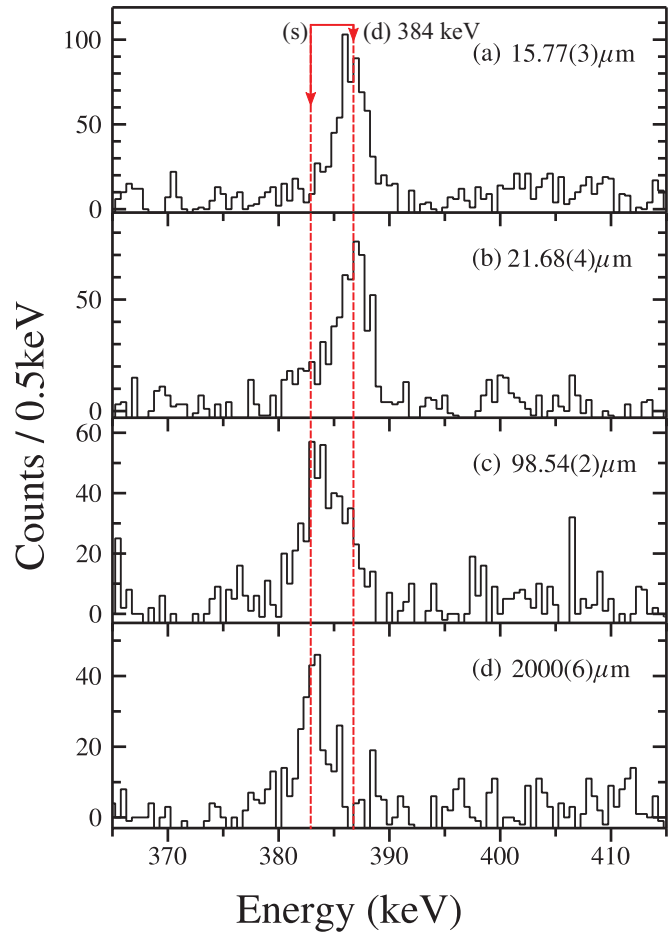

FIG. 4. (Color online) Example of recoil-gated γ-γ coincidence spectra for four target-to-degrader distances for the 384-keV transition in the ground-state band of ^{138}Gd. The spectra were obtained from a summation of gates across the full photo-peak widths of the 556- and 616-keV γ rays. The splitting of the fully Doppler-shifted (s) and degraded (d) components is highlighted.

solely fed by the 384-keV γ-ray transition depopulating the 4^+ state in the ground-state band. This work supports that conclusion because a weighted average of intensity ratios for the two transitions at each target-to-degrader distance, corrected for efficiency, was found to be $\alpha = 1.03(2)$. In this work, the error on each lifetime measurement $\tau(d)$ was determined by the absolute values of intensities measured at each distance. This includes the effects resulting from the small separation of the fully Doppler-shifted and degraded components of the full photo peaks for low-energy transitions, such as the 221-keV γ ray (see Fig. 2). The normalized fully Doppler-shifted intensities for each transition in ^{138}Gd measured in this work for ^{138}Gd are shown in Fig. 3.

Figure 4 shows example spectra for the 384-keV transition depopulating the 4^+ state in ^{138}Gd as measured in this work. The spectra were obtained from a summation of gates on the higher lying 556- and 616-keV transitions. Because of similar coincident energies in ^{138}Gd with transitions in ^{138}Eu [25], produced with a relative cross section of 46%, no further gates could be placed on higher spin transitions in the ^{138}Gd yrast sequence. The lifetime deduced for the 4^+ state in ^{138}Gd in this work is significantly larger than that measured by Bishop *et al.* [12]; see Table I. Similar to the calculation of the 2^+ state, Bishop *et al.* [12] made assumptions as to the properties of the transitions feeding the 4^+ state. In that case, the feeding properties of the 6^+ state, which assumed a constant deformation with increasing spin up the yrast band, were included in the analysis for the 4^+ state. These assumptions had the effect of reducing the measured lifetime of the 6^+ state from its upper limit of 13.7(16) ps to 7(2) ps, the consequence of which was a reduced value for the lifetime of the 4^+ state [12]. The present work has managed to more accurately account for the properties of the 489-keV transition feeding the 4^+ state in ^{138}Gd, through the use of γ-ray coincidences, by removing any contributions from observed and unobserved side feeding.

Similar spectra were analyzed in order to determine the lifetimes of the 6^+ and 8^+ states in ^{138}Gd. The lifetime of the 6^+ state was calculated using a gate on the higher lying 616-, 762-, and 838-keV transitions. No further gates were able to be used due to the presence of the 554-keV γ ray in ^{139}Eu [28] overlapping with the 556-keV transition in ^{138}Gd. The lifetime measurement of 3.8(15) ps determined for this state is in agreement with that found in Ref. [12]. The excited 8^+ state in ^{138}Gd was analyzed with a sum of gates placed on the 762-, 838-, 969-, and 1013-keV transitions (see Ref. [25]). The more intense 686-keV γ ray was excluded from the gate because of its presence in ^{139}Eu [28]. It was not possible to measure the lifetimes of any higher lying states in this work because of insufficient statistics.

TABLE II. Experimentally measured excitation energy ratios for ^{138}Gd [25] and values determined from X(5) and IBM-1 theoretical calculations. Values are given relative to the energy of the first excited 2^+ state.

	$E(J_1^+)/E(2_1^+)$		
J^π	Exp.	X(5)	IBM-1
2^+	1	1	1
4^+	2.74	2.91	2.36
6^+	4.95	5.45	4.09
8^+	7.47	8.51	6.14

TABLE III. Experimental and theoretical $B(E2)$ values for excited yrast states in ^{138}Gd measured in this work. All $B(E2)$ values have been normalized to the $B(E2; 2_1^+ \rightarrow 0_1^+)$ ground-state transition.

	$B(E2; J \rightarrow J-2)/B(E2; 2_1^+ \rightarrow 0_1^+)$			
J^π	Exp.	IBM-1	X(5)	PES[a]
2^+	1.0(1)	1.0	1.0	1.0
4^+	1.6(2)	1.8	1.6	1.8
6^+	1.7(7)	2.2	2.0	2.0
8^+	1.9(5)	2.4	2.3	2.2

[a]Values determined from quadrupole moments derived from PES calculations, under the assumption of a prolate-deformed nucleus.

IV. DISCUSSION

Several experimental properties of nuclei can be used to assess the potential of phase-transitional behavior. These include the ratio of the product and sum of the number of valence protons (N_p) and valence neutrons (N_n), known as the P factor [8]:

$$P = \frac{N_p N_n}{N_p + N_n}. \quad (2)$$

A value of $P \sim 5$ describes the point where the strength of the p-n interaction ($N_p N_n$) begins to dominate over the pairing interaction ($N_p + N_n$) [1]. A P value of 5.1 is calculated for ^{138}Gd, which may suggest that it could exhibit phase-transitional behavior. Another measure of transitional behavior in nuclei are the experimental energy ratios $E(J_1^+)/E(2_1^+)$. Table II shows the experimental energy ratios in ^{138}Gd compared with predictions from X(5) and IBM-1 calculations. Both the experimental measurements and the calculations allow the possibility that ^{138}Gd may show X(5) behavior in its low-lying structure. The most definitive test of possible X(5) critical-point behavior relies on knowing the lifetimes of excited states, which is the focus of the present work. The experimentally measured lifetimes for the ground-state band in ^{138}Gd have been related to the reduced transition probability by

$$\tau = \frac{0.082}{B(E2; I \rightarrow I-2)(1+\alpha_{\rm tot})E_\gamma^5}, \quad (3)$$

where τ is in picoseconds, E_γ is in MeV, and $B(E2)$ is in e^2b^2. The total internal conversion coefficient, $\alpha_{\rm tot}$, was taken from Ref. [29]. In order to interpret the low-lying collective structure of ^{138}Gd, the experimentally derived $B(E2)$ values have been compared with three different sets of theoretical calculations: X(5), IBM-1, and PES. The reduced transition probabilities determined experimentally and those predicted from each of the theoretical calculations are shown in Table III.

The X(5) critical-point symmetry calculations discussed in this work are taken from the solutions to the Bohr Hamiltonian, adopting an infinite square well and harmonic oscillator potential approximation for the decoupled β and γ degrees of freedom, respectively [5]. This Hamiltonian is analytically solvable and provides parameter-free (except for scale) solutions for both energies and transition probabilities for excited nuclear states at the critical point of a phase transition [4,5]. The $B(E2)$ values determined from this model are shown in Table III. Figure 5 compares the experimentally deduced normalized transition probabilities with the results from X(5) calculations, as well as those from the standard vibrational and rigid-rotor paradigms [30].

Although the large uncertainties associated with the experimentally measured $B(E2)$ values cannot rule out contributions for rotational and vibrational modes of excitation, it is clear that ^{138}Gd may lie near the critical point. It should be noted that X(5) calculations are parameter free and do not allow any contributions from γ softness in the potential, or indeed deviations from axial symmetry. Recent lifetime measurements for the rare-earth nucleus ^{130}Ce were able to attribute deviations from the X(5) model to a structure intermediate between an axially symmetric and γ-soft potential in the γ degree of freedom [10]. This approach was guided by the observation of γ-vibrational bands at low excitation energies with respect to the ground state. Similar low-energy excited 2^+ states have been observed in many of the $N = 74$ isotones [31–34] but not to date in ^{138}Gd. In order to further assess possible deviations of the low-lying structure in ^{138}Gd from X(5) behavior, IBM-1 calculations have been performed at the critical point.

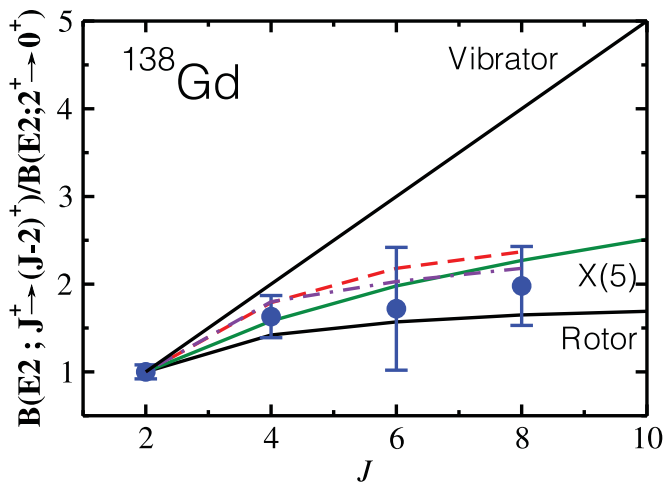

FIG. 5. (Color online) Comparison of experimental normalized $B(E2)$ values with those calculated from vibrational and rotational paradigms, as well as the X(5) (solid green line), IBM-1 (dashed line), and PES (dash-dot line) calculations.

Two-parameter IBM-1 calculations have been performed at the critical point using the Hamiltonian

$$\hat{H} = C[(1-x)\hat{n}_d - (x/4N_b)\hat{Q}_\chi \cdot \hat{Q}_\chi], \quad (4)$$

where C is a normalization constant that scales with energy. The d-boson number operator is given by $\hat{n}_d = d^\dagger \cdot \tilde{d}$ and the quadrupole operator $\hat{Q}_\chi$ is defined as

$$\hat{Q}_\chi = [d^\dagger_\mu s + s^\dagger \tilde{d}_\mu]^{(2)} + \chi[d^\dagger_\mu \times \tilde{d}_\mu]^{(2)}. \quad (5)$$

The number of bosonic pairs was determined with respect to the nearest closed shells, seven proton pairs above the $Z = 50$ shell closure and four neutron-hole pairs below the $N = 82$ shell gap, giving $N_b = 11$. The value of χ was taken as that for the SU(3) case, $-\sqrt{7}/2$. Variations in x from 0 to 1 correspond to the transition from sphericity to an axially symmetric nuclear shape. The critical point occurs at $x_{\rm crit} = 16N_b/(34N_b - 27) = 0.508$. Figure 5 (dashed line) and Table III show the deduced $E2$ electromagnetic transition strengths calculated from the IBM-1 model.

The IBM-1 calculations at the critical point predict that ^{138}Gd should exhibit a slightly more vibrational component at low spin compared with the X(5) prediction; see Fig. 5. The experimentally deduced $B(E2)$ values in this work are consistent with such a description; however, the large uncertainties cannot determine the extent to which vibrations and rotations contribute to the structure of ^{138}Gd.

In order to proceed with the interpretation of the experimentally measured $B(E2)$ values in ^{138}Gd, it is necessary to examine the effects of the γ degree of freedom on the measured values. The X(5) and IBM-1 calculations performed in this work for ^{138}Gd are not sensitive to an influence from a γ-soft nuclear potential. However, the more recent work on X(5) critical point calculations of Caprio [35] was able to determine exact solutions to the Bohr Hamiltonian, obtaining the X(5) result, without the approximate separation of the β and γ variables as used in Ref. [5]. The calculations from Caprio highlighted the effects from the β-γ coupling, particularly through the presence of substantial dynamical γ softness [35]. In order to assess the effects of the γ degree of freedom on the $B(E2)$ values measured in this work, PES calculations have been performed for increasing rotational frequency in the ground-state band of ^{138}Gd. The PES calculations were performed using the configuration-constrained blocking method, where single-particle orbitals were kept singly occupied as the deformation was varied [36,37]. The single-particle orbitals were determined from a set of average Nilsson numbers, $\langle N\rangle$, $\langle n_z\rangle$, $\langle\Lambda\rangle$, and $\langle|\Omega|\rangle$ for the ground-state configuration in ^{138}Gd. The PESs were calculated for a range of rotational frequencies at quadrupole deformation (β_2, γ) with hexadecapole (β_4) variation. Figure 6 shows the PES predictions for ^{138}Gd following the ground-state configuration through increasing rotational frequencies. These plots reveal any potential γ softness from the apparent width of the calculated minima. Table IV summarizes the deformation parameters calculated for each excited level in ^{138}Gd.

The $E2$ electromagnetic transition strengths were determined from the PES calculations using the simple

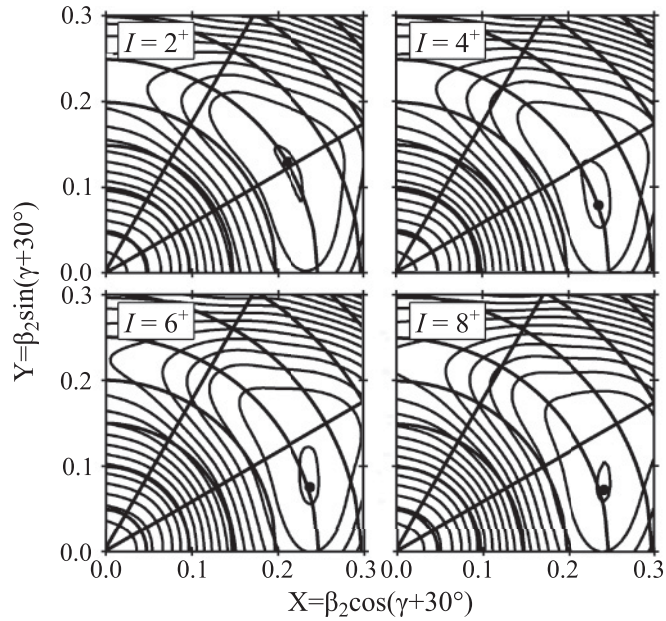

FIG. 6. Calculated PESs following the ground-state configuration in ^{138}Gd for increasing rotational frequency. Each panel is labeled by the corresponding spin and parity of the excited level at that angular momentum. The evolution of the absolute minimum toward a more axially asymmetric shape can clearly be seen with increasing rotational frequency. A significant amount of γ softness can also be seen at each rotational frequency.

rotational-model relationship [30]

$$B(E2; I \to I-2) = \frac{5}{16\pi} Q_t^2 \langle I\,K\,20|I-2K\rangle^2, \quad (6)$$

where

$$Q_t = Q_{20} + \sqrt{\frac{2}{3}} Q_{22}. \quad (7)$$

Equation (7), taken from Ref. [38], allows the determination of Q_t from the components Q_{20} and Q_{22}, calculated macroscopically from the values β and γ, derived from the PES calculations. This prescription for the quadrupole moments allowed the inclusion of γ degrees of freedom in the final predicted $B(E2)$ values. The normalized $B(E2)$ values derived from the PES calculations are shown in Fig. 5 (dot-dashed line). For the low-spin levels, the calculations show a trend similar to those of the IBM-1 calculations, where ^{138}Gd is initially predicted to exhibit properties with a slightly more vibrational component than an axially symmetric rotor component. However, for increasing spin, the PES predictions deviate from those calculated using the IBM-1 model and appear to cross the critical-point ratio toward the behavior described by a rotor. The PES plots shown in Fig. 6 highlight the significant amount of γ softness for each of the excited states of ^{138}Gd measured in this work. Based upon these results, any possible deviation between the experimentally measured reduced transition probabilities and values predicted by X(5) may be a consequence of the contribution from γ degrees of freedom. This hypothesis is supported by the presence of low-lying γ-vibrational bands in the $N = 74$ isotones [32–34],

TABLE IV. Variation of deformations and quadrupole moments for the ground-state band in ^{138}Gd determined from theoretical PES calculations based upon the configuration-constrained blocking method [36,37].

J_i^π	β_2	γ°	Q_t
2^+	0.25	1	5.91
4^+	0.25	−12	6.62
6^+	0.25	−13	6.72
8^+	0.26	−13	6.82

although the exact excitation of the band-head state is not known in ^{138}Gd. In order to examine the effects of a more γ-soft potential, IBM-1 calculations are required where the value of χ, governing the degree of γ softness, is allowed to vary.

Figure 5 highlights the increasing separation with spin between the values expected from the X(5) and the rotational and vibrational paradigms. Consequently, it would be desirable to measure lifetimes for higher spin values. However, it should be noted that the ground-state band in ^{138}Gd is crossed by a more aligned band in the first band crossing [25]. The continuation of the nonyrast ground-state band configuration is currently unknown in ^{138}Gd. This is in contrast to the states analyzed in ^{152}Sm, which follow the ground-state configuration with increasing spin through the first crossing [39]. In ^{138}Gd, the mixing of the ground-state and aligned bands would be expected to modify the lifetimes of the excited states. In order to more fully assess the potential X(5) behavior at higher spin, the known level scheme of the ground-state band in ^{138}Gd needs to be extended to the nonyrast sequence above the first band crossing. Furthermore, the identification of excitation energies for the low-spin γ and β-vibrational bands in ^{138}Gd would help to experimentally characterize the susceptibility of the nucleus to γ and β distortions. In summary, $B(E2)$ measurements for excited states in the ground-state band sequence, measured in this work, cannot fully rule out the possibility that ^{138}Gd shows X(5) critical-point behavior. Further experimental measurements of excited states in ^{138}Gd, as well as lifetime measurements with reduced uncertainties, are required to fully explore this possibility.

V. CONCLUSIONS

In conclusion, lifetime measurements have been made for the first four excited states in the ground-state band of ^{138}Gd using the recoil-distance Doppler-shift method. Data were collected using the Köln plunger at the target position of the JUROGAM-II γ-ray spectrometer at the University of Jyväskylä, Finland and analyzed using the DDCM in the γ-ray coincidence mode. The large errors associated with the experimentally derived $B(E2)$ values prevent ^{138}Gd from being definitively placed near the X(5) critical point. PES calculations allude to a significant degree of γ softness in the low-lying structure of ^{138}Gd, which is not accounted for in either the X(5) or IBM-1 calculations performed in this work. This increased susceptibility to γ-vibrational excitations in ^{138}Gd is thought to significantly contribute toward the low-lying structure of ^{138}Gd and may explain the possible deviations from the X(5) critical-point description. Further analysis into the exact structure of the γ and β vibrational bands is required to fully understand the structure of ^{138}Gd, as well as more accurate lifetime measurements of the ground-state band levels.

ACKNOWLEDGMENTS

This work has been supported by the EU 7th Framework Programme, "Integrating Activities—Transnational Access," Project No. 262010 (ENSAR), and by the Academy of Finland under the Finnish Centre of Excellence Programme 2006-2011 (Nuclear and Accelerator-Based Physics Programme at JYFL). The authors acknowledge the support of GAMMAPOOL for the loan of the JUROGAM detectors. M.G.P., D.M.C., and M.J.T. acknowledge the support of the STFC. P.T.G. acknowledges the support of the Academy of Finland through Contract No. 119290.

[1] R. F. Casten, Nat. Phy. **2**, 811 (2006).
[2] R. F. Casten and E. A. McCutchan, J. Phys. G: Nucl. Part. Phys. **34**, R285 (2007).
[3] P. Cejnar, J. Jolie, and R. F. Casten, Rev. Mod. Phys. **82**, 2155 (2010).
[4] F. Iachello, Phys. Rev. Lett. **85**, 3580 (2000).
[5] F. Iachello, Phys. Rev. Lett. **87**, 052502 (2001).
[6] R. F. Casten and N. V. Zamfir, Phys. Rev. Lett. **87**, 052503 (2001).
[7] R. Krücken *et al.*, Phys. Rev. Lett. **88**, 232501 (2002).
[8] R. F. Casten, D. S. Brenner, and P. E. Haustein, Phys. Rev. Lett. **58**, 658 (1987).
[9] R. B. Cakirli and R. F. Casten, Phys. Rev. Lett. **96**, 132501 (2006).
[10] A. F. Mertz *et al.*, Phys. Rev. C **77**, 014307 (2008).
[11] C. J. Lister *et al.*, Phys. Rev. Lett. **55**, 810 (1985).
[12] P. J. Bishop *et al.*, J. Phys. G **14**, 995 (1988).
[13] P. T. Greenlees *et al.*, AIP Conf. Proc. **764**, 237 (2005).
[14] M. Leino, Nucl. Instrum. Methods Phys. Res., Sect. B **126**, 320 (1997).
[15] M. Leino *et al.*, Nucl. Instrum. Methods Phys. Res., Sect. B **99**, 653 (1995).
[16] R. D. Page *et al.*, Nucl. Instrum. Methods Phys. Res., Sect. B **204**, 634 (2003).
[17] P. T. Greenlees *et al.*, Eur. Phys. J. A **25**, 599 (2005).
[18] A. Dewald *et al.*, Nucl. Phys. A **545**, 822 (1992).
[19] I. Lazarus *et al.*, IEEE Trans. Nucl. Sci. **48**, 567 (2001).
[20] P. Rahkila, Nucl. Instrum. Methods Phys. Res., Sect. A **595**, 637 (2008).
[21] W. T. Milner (private communication).
[22] A. Dewald, S. Harissopulos, and P. von Brentano, Zeitschrift für Physik A Hadrons and Nuclei **334**, 163 (1989).

[23] G. Böhm, A. Dewald, P. Petkov, and P. von Brentano, Nucl. Instrum. Methods **329**, 248 (1993).
[24] A. Dewald *et al.*, Phys. Rev. C **68**, 034314 (2003).
[25] E. S. Paul *et al.*, J. Phys. G: Nucl. Part. Phys. **20**, 751 (1994).
[26] R. Ma *et al.*, Phys. Rev. C **40**, 156 (1989).
[27] R. Ma *et al.*, J. Phys. G: Nucl. Part. Phys. **16**, 1233 (1990).
[28] P. Vaska *et al.*, Phys. Rev. C **52**, 1270 (1995).
[29] A. A. Sonzogni, Nucl. Data Sheets **98**, 515 (2003).
[30] A. Bohr and B. R. Mottelson, *Nuclear Structure* (Benjamin, New York, 1975), Vol. 2.
[31] S. Xiangfu *et al.*, Phys. Rev. C **28**, 1167 (1983).
[32] E. S. Paul *et al.*, Phys. Rev. C **36**, 2380 (1987).
[33] E. S. Paul *et al.*, J. Phys. G: Nucl. Part. Phys. **19**, 861 (1993).
[34] E. S. Paul *et al.*, Nucl. Phys. A **619**, 177 (1997).
[35] M. A. Caprio, Phys. Rev. C **72**, 054323 (2005).
[36] F. R. Xu, P. M. Walker, J. A. Sheikh, and R. Wyss, Phys. Lett. B **435**, 257 (1998).
[37] F. R. Xu, P. M. Walker, and R. Wyss, Phys. Rev. C **59**, 731 (1999).
[38] R. W. Laird *et al.*, Phys. Rev. Lett. **88**, 152501 (2002).
[39] J. Konijn *et al.*, Nucl. Phys. A **373**, 397 (1982).